Journal of Environmental Management 316 (2022) 115275

Contents lists available at ScienceDirect

Journal of Environmental Management

journal homepage: www.elsevier.com/locate/jenvman

Research article

# Characterization and nutritional value of hydrothermal liquid products from distillers grains

Qingya Xu [a,b], Taoze Liu [a,*], Bangyu Liu [c,**], Hongguang Cheng [b], Cheng Yang [a], Bing Wang [d], Andrew R. Zimmerman [e], Bin Gao [f]

[a] College of Eco-Environmental Engineering, Research Center of Solid Waste Pollution Control and Recycling, Guizhou Minzu University, Guiyang, 550025, Guizhou, China
[b] State Key Laboratory of Environmental Geochemistry, Institute of Geochemistry, Chinese Academy of Sciences, Guiyang, 550081, Guizhou, China
[c] College of Architectural Engineering, Research Center of Solid Waste Pollution Control and Recycling, Guizhou Minzu University, Guiyang, 550025, Guizhou, China
[d] College of Resources and Environment Engineering, Guizhou University, Guiyang, 550025, Guizhou, China
[e] Department of Geological Sciences, University of Florida, Gainesville, FL, 32611, USA
[f] Department of Agricultural and Biological Engineering, University of Florida, Gainesville, FL, 32611, USA

ARTICLE INFO

*Keywords:*
Distillers grains
Hydrothermal liquid products
Hydrothermal treatment
Nutrients

ABSTRACT

Hydrothermal liquid products (HLPs) produced by hydrothermal treatment (HTT) contain a large amount of nitrogen, phosphorus and other substances, while the environmental problems caused by arbitrary discharge. This work explored the effects of temperature, reaction time and solid-liquid ratio on the chemistry of HLPs of two different distillers grains, with a focus on nutrient composition. Increased HTT temperature was related to increased HLPs pH, dissolved organic carbon content, and aromaticity, and decreased electrical conductivity. Maximum nutrient extraction efficiencies observed for $NH_4^+$-N, $NO_3^-$-N and $PO_4^{3-}$ were 92.0, 89.9, and 94.3%, respectively. Response surface methodology showed that the release of nutrient extraction efficiency was the greatest at the hydrothermal treatment of 200 °C for 1 h, and using a solid/liquid ratio of 10%. Comparative studies, the nutritional value of HLPs are appropriate for use as an agricultural fertilizer, and its use as a substitute for synthetic fertilizers could increase the sustainability and profitability of farming.

## 1. Introduction

Distillers grains are by-products of the cereal distillation process with huge water content and difficult to deal with (JoelReyes-Cabrera, 2017; Yujia Xiang, 2020). Hydrothermal treatment (HTT) of distillers grains is a new method to treat wet organic matter. (Li et al., 2020; Lima et al., 2017). Many studies have focused on the solid products of HTT, including energy sources (Ramesh et al., 2019), soil amendments (Huang et al., 2019; Kumar, 2020) or sorbent materials (Li et al., 2019; Nascimento et al., 2009). With the production of high value-added solid products, hydrothermal liquid products (HLPs) may become a secondary pollution source. Water is the main medium in the HTT, most of the transformation is carried out in the aqueous phase, and the generated HLPs contains a lot of nitrogen, phosphorus and organic matter. Therefore, HLPs is a potential resource, and direct discharge may cause water bodies eutrophication.

However, research into HTT conditions is conducive to understanding the changes in the physicochemical properties of hydrothermal liquid phase, exploring its potential utilization value, and reducing the above-mentioned environmental problems. Reza et al. (2014) found that concentrations of a variety of sugars, acids, and furfurals in pine wood HLPs were maximized at 200 °C for 5 min HTT. Köchermann et al. (2018) showed that HTT conditions, including temperature, residence time and solid-liquid ratio, controlled the content of organic acids and other substances in hydrochar and were helpful in getting the value product. Temperature has been found to be one of the most important factors influencing the HTT of biomass (Román et al., 2020; T. Wang et al., 2020), and focus on the hydrothermal temperature effected on the nutrients release in HLPs. For example, Yu et al. (2017) found that the HTT at 200 °C for 30 min released more phosphate and ammonium than higher temperatures. This illustrates the HLPs characteristics are substantially different depending on the feedstocks and HTT process

* Corresponding author.
** Corresponding author.
*E-mail addresses:* liutaoze@foxmail.com (T. Liu), liubangyu1982@126.com (B. Liu).

https://doi.org/10.1016/j.jenvman.2022.115275
Received 26 January 2022; Received in revised form 7 May 2022; Accepted 7 May 2022
Available online 20 May 2022
0301-4797/© 2022 Elsevier Ltd. All rights reserved.

variables. The major process variables controlling HLPs characteristics are temperature, residence time and solid-liquid ratio.

In addition, the type of feedstock used may also be closely related to the nutrient composition of HTT products (He et al., 2015). Li et al. (2020) showed that the different raw materials affected total recoverable energy and hydrochar yields. Ekpo et al. (2016) found that the nutrient content of hydrothermal products was related to the existence of inorganic elements such as calcium and magnesium in the feedstock. Vermiculite, as a non-toxic and harmless clay mineral, contains inorganic substances such as Mg, Al, Fe and so on (Ma et al., 2019; Pisa et al., 2020), which may changes the characteristics of hydrothermal products. In previous studies, Xu et al. (2021) found that the hydrochar structure was changed and surface active functional and groups absorption efficiency were increased by co-hydrothermal carbonization with Vermiculite. Clay minerals can affect the leaching and transformation of nutrients and the passivation actions (Mazloomi and Jalali, 2019). Therefore, the research needs to focus on exploring the role of added vermiculite in HTT.

However, up to now, there are few studies on recovery of distillers grains HLPs after HTT. It is expected that these nutrients can be recycled for plant growth to improve the overall economic benefits of the distillers grains HTT. Here, the effects of HTT temperature, duration, and solid/liquid ratio on the chemistry of HLPs of distillers grains were examined, along with the effects of the addition of vermiculite. Response surface methodology (RSM), which explores the relationships between several explanatory variables, was used to identify the HTT conditions that would produce maximal HLPs inorganic nutrients ($NH_4^+$-N, $NO_3^-$-N, $PO_4^{3-}$). Finally, the generated results were compared with those from several previous studies to assess the potential of HLPs for use as an agricultural fertilizer. Thus, the paper will provide new solutions to efficiently treat HLPs.

## 2. Materials and methods

### 2.1. Materials

Distillers grains were obtained from a grain distillery in Guizhou Province, P. R. China that uses glutinous sorghum and wheat grain (designated DG I), the moisture content of about 60%. A second distillers grains (DG II), the moisture content is about 50%, were obtained from a brewery in Guizhou Province, P. R. China that uses barley malt grain. Vermiculite ($AlFeMgO_3Si$), with a particle size between 0.1 and 0.15 mm, was purchased from Shanghai McLean Biochemical Technology Co., Ltd. Vermiculite, as a clay mineral, can change the characteristics of hydrothermal products and has passivation. Other chemicals used were of analytical grade and did not require further purification. Ultrapure water (water purifier UPC-10T, ULUPURE, CHINA) was used throughout the experiments.

### 2.2. Hydrothermal reaction process

Distillers grains samples were weighed and transferred to a 1500 mL reaction kettle (GSHA, JIAYI, CHINA) where they were mixed with ultrapure water. Three feedstocks DG I, DG II and DG I with 5% (v/v%) vermiculite, by weight (DG-V5%) were examined. For each, HTT was carried out at three temperatures (100, 150, and 200 °C), three duration period (1, 3.5 and 6 h), and using three solid/liquid weight ratios (5, 10, and 15%). During the hydrothermal process, a magnetic stirring speed was maintained at 100 rpm. After the reaction and cooling to room temperature, the solid and liquid were separated using a 0.45 μm nylon membrane filter (Whatman 1004–055, USA). The liquid products were stored in a refrigerator at 4 °C until further analysis. Each HTT experiment was performed three times.

### 2.3. Chemical analyses

The pH value and electrical conductivity (EC) of HLPs were measured by pH meter (PHS-25, LEICI, CHINA) and electrical conductivity meter (DDSJ-318, LEICI, CHINA), respectively. Dissolved organic carbon (DOC) in HLPs was determined using a total organic carbon analyzer (Aurora iTOC 1030W, OI, U.S.). The inorganic nutrients ($NH_4^+$-N, $NO_3^-$-N and $PO_4^{3-}$) in HLPs were quantified using an automated wet chemical analyzer with continuous flow analysis (Skalar Analytical, Skala, Netherlands). Each measurement was repeated 3 times, and the mean value and standard deviation were reported here. Organic component distributions in HLPs were compared using three-dimensional excitation-emission matrix (EEM) fluorescence spectroscopy (F-7000, Hitachi, Japan). The scanning rate was set at 240 nm $min^{-1}$. The excitation wavelength ($E_x$) ranged from 250 nm to 460 nm and the emission wavelength ($E_m$) ranged from 240 nm to 440 nm. Refer to common wavelength ranges (Katsuyama and Ohte, 2002; Wang et al., 2009).

### 2.4. Quantitative treatment of data

The nutrient release efficiencies (R) for $NH_4^+$-N, $NO_3^-$-N and $PO_4^{3-}$ from distillers grains during HTT were calculated as follows (Sumida H and Sumida, 2013):

$$R(\%) = \left(m_f - m_o\right) / m_o \times 100\% \quad (1)$$

where $m_f$ *and* $m_0$ (mg) is the mass of $NH_4^+$-N, $NO_3^-$-N and $PO_4^{3-}$ in the liquid phase of distillers grains after HTT and in the distillers grains used in the experiment before HTT, respectively.

Principal component analysis (PCA) is a mathematical procedure that reduces the dimensionality of a dataset by grouping together variables that are autocorrelated, thus can be treated as one variable (Oliveira et al., 2020). In this experiment, there are three indicators ($NH_4^+$-N, $NO_3^-$-N, $PO_4^{3-}$) that are related to inorganic nutrient content but cannot be added directly. In order to establish a relationship between $NH_4^+$-N, $NO_3^-$-N, $PO_4^{3-}$ in distillers grains HLPs and HTT conditions, The concentrations of $NH_4^+$-N, $NO_3^-$-N and $PO_4^{3-}$ in liquid products were PCA and normalized (the original data in Table S1, Supplementary material) using SAS 9.3 software (SAS Institute Inc., North Carolina, USA). The relevant data PCA (Minoglou and Komilis, 2018) was established to Fq. (2):

$$C_{PC} = 0.8437 \times C_{NH} + 0.1448 \times C_{NO} + 0.0115 \times C_P \quad (2)$$

where $C_{PC}$ is the new principal component representing nutrients in the HLPs, mg $L^{-1}$; and $C_{NH}$ $C_{NO}$ and $C_P$ are concentrations of $NH_4^+$-N, $NO_3^-$-N and $PO_4^{3-}$ in HLPs (mg $L^{-1}$), respectively.

Response surface methodology (RSM) are graphical representations used to describe the interactive effects of process variables and their effects on a response variable. RSM is often used to determine the optimal experimental conditions to maximize a specific response. In this study, RSM was used to identify optimal HTT conditions (temperature, duration period and liquid/solid weight ratio) for maximal extraction of HLPs inorganic nutrients from DG I. Based on the Design Expert 10.0.1 software (Stat-Ease, Minneapolis, MN, USA), a Box-Behnken design (BBD) was used to study the three-parameter interactions, over 17 HTT runs (i.e. HTT condition combinations). The mathematical relationship between the three experimental parameters can be approximated by a second order polynomial model (Sharma et al., 2020):

$$Y = \beta_0 + \sum_{i=1}^{3} \beta_i X_i + \sum_{i=1}^{3} \sum_{j=1}^{3} \beta_{ij} X_i X_j + \sum_{i=1}^{3} \beta_{ii} X_i^2 + \varepsilon \quad (3)$$

where Y is the model response, $\beta_0$ is the coefficient of the intercept, $\beta_i$ is the coefficient of the linear effect, $\beta_{ii}$ is the coefficient of the quadratic effect, $\beta_{ij}$ is the coefficient of the interaction effect, $X_i$ and $X_j$ are pre-

dicted variables for the independent factors, and $\varepsilon$ is a random error term. Then, analysis of variance (ANOVA) was used to fit the regression model and evaluate its significance.

## 3. Results and discussion

### 3.1. Chemical characteristics of HLPs

#### 3.1.1. pH, electrical conductivity (EC) and DOC of HLPs

All the HLPs were acidic, ranging from pH 3.9 to 5.0 (Table 1), and increased with HTT temperature. This increase can be attributed, either to the production and release of organic acids via thermal degradation during HTT (Lucas Raimundo Bento et al., 2020; Sumida H and Sumida, 2013) or to greater release of ammonium salt and other alkaline products at higher temperatures (Wu et al., 2018). The addition of vermiculite, solid/liquid ratio, and HTT duration had no significant effect on the pH of the liquid products. The pH of DG II LHPs were generally higher than those of DG I.

The EC has been used as a proxy for the dissolved salt content in a sample (Xiong et al., 2019). The EC of the HLPs decreased sharply with increasing HTT temperature and decreased a smaller amount with increasing HTT duration (Table 1). The reason for this may be that, with increasing HTC temperature and duration, more organic solutes were released into solution (see below), which can bind with inorganic ions, reducing the electrical conductivity of the HLPs. Alternatively, according to previous research (Xu et al., 2021), a large number of ions become enriched on the hydrochar surface as HTT progresses, reducing their transfer to the liquid phase.

With rising HTT temperature, the content of DOC increased sharply (Table 1), likely because dehydration and decarboxylation reactions begin to fragment hemicellulosic biomass, releasing organic monomers to solution. Cellulose has been shown to begin to break down at 200 °C (Jaruwat et al., 2018) and lignin over a broader temperature range (Kawamoto, 2017). With increasing HTT residence times, the slight decrease in DOC may be explained by the occurrence of polymerization of dissolved fragments and recondensation back to solid hydrochar (Wang et al., 2018). The significant decrease in HLPs DOC content with increasing liquid-solid ratio can easily be explained as a dilution effect.

Regardless of HTT temperature, the HLPs DOC contents from the three feedstocks were as follows: DG I > DG II > DG-V5% (Table 1). The highest DOC content observed was 1793.7 mg $L^{-1}$ from DG I produced at 200 °C, 1 h, liquid-solid ratio = 10). In addition, when vermiculite was added in the hydrothermal process, the DOC content of the liquid products decreased, which might be because vermiculite acted as a passivator, shielding the outer layer of hydrochar from dissolution. It also may have adsorbed released DOC components.

#### 3.1.2. HLPs three-dimensional EEM fluorescence spectroscopy characteristics

The fluorescence excitation emission matrix produced by DG-V15% HLPs produced at 150 °C (Fig. 1) displayed features similar to those of other HLPs (Fig. S1, Supplementary material). According to previous studies, three-dimensional fluorescence spectra can be divided into five regions, which identify dominant fluorescent organic matter types, namely: tyrosine/tryptophan (I, Em 220–240 nm/Ex280-360 nm);

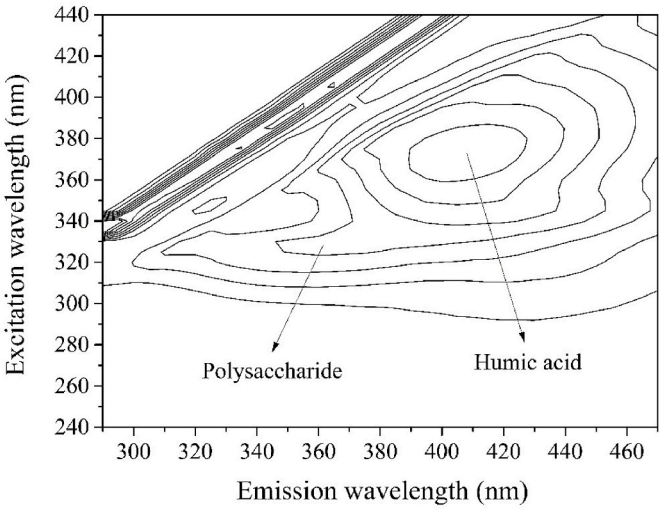


**Fig. 1.** Fluorescence excitation emission matrix and fluorophore fields identified in DG-V5% HLPs produced at 150 °C, 1 h, 10% solid/solution ratio.

**Table 1**
Characteristics of hydrothermal liquid products under different hydrothermal treatment conditions.

| Hydrothermal carbonation conditions | | | | pH | Conductivity (ms $cm^{-1}$) | DOC (mg $L^{-1}$) |
|---|---|---|---|---|---|---|
| Raw material | Temperature (°C) | Duration (h) | Solid/liquid ratio (%) | | | |
| DG I | 100 | 1 | 10 | 3.92 ± 0.03 | 1016 ± 1.7 | 520.1 ± 2.7 |
| | 150 | 1 | 10 | 4.13 ± 0.02 | 145 ± 1.2 | 1156.1 ± 3.2 |
| | 200 | 1 | 10 | 4.27 ± 0.11 | 5.9 ± 0.3 | 1794.2 ± 2.9 |
| | 200 | 3.5 | 10 | 4.36 ± 0.08 | 4.0 ± 0.4 | 1607.2 ± 3.4 |
| | 200 | 6 | 10 | 4.43 ± 0.04 | 2.8 ± 0.5 | 1494.7 ± 3.6 |
| | 200 | 6 | 5 | 4.42 ± 0.03 | 5.8 ± 0.7 | 1647.7 ± 2.2 |
| | 200 | 6 | 15 | 4.58 ± 0.01 | 2.1 ± 0.4 | 1298.9 ± 4.3 |
| DG-V5% | 100 | 1.0 | 10 | 4.12 ± 0.07 | 1599 ± 2.4 | 421.5 ± 2.8 |
| | 150 | 1.0 | 10 | 4.21 ± 0.13 | 112 ± 1.3 | 925.7 ± 4.5 |
| | 200 | 1.0 | 10 | 4.27 ± 0.06 | 3.7 ± 0.3 | 1573.2 ± 3.2 |
| | 200 | 3.5 | 10 | 4.43 ± 0.08 | 3.5 ± 0.4 | 1435.8 ± 2.8 |
| | 200 | 6.0 | 10 | 4.57 ± 0.14 | 2.7 ± 0.4 | 1165.3 ± 3.1 |
| | 200 | 6.0 | 5 | 4.49 ± 0.08 | 3.6 ± 0.7 | 1375.4 ± 2.6 |
| | 200 | 6.0 | 15 | 4.51 ± 0.07 | 3.2 ± 0.5 | 1123.2 ± 4.1 |
| DG II | 100 | 1.0 | 10 | 4.93 ± 0.02 | 584 ± 1.4 | 155.2 ± 2.7 |
| | 150 | 1.0 | 10 | 5.02 ± 0.09 | 88.5 ± 1.3 | 1043.1 ± 3.1 |
| | 200 | 1.0 | 10 | 4.97 ± 0.11 | 2.6 ± 0.1 | 1676.6 ± 3.3 |
| | 200 | 3.5 | 10 | 5.15 ± 0.06 | 2.3 ± 0.3 | 1460.4 ± 4.6 |
| | 200 | 6.0 | 10 | 5.05 ± 0.07 | 2.4 ± 0.3 | 1283.3 ± 3.6 |
| | 200 | 6.0 | 5 | 4.92 ± 0.07 | 2.5 ± 0.2 | 1335.6 ± 2.9 |
| | 200 | 6.0 | 15 | 5.03 ± 0.12 | 2.5 ± 0.5 | 1210.5 ± 2.6 |
| DG I P-value | Temperature | | | 0.004 | 0.476 | 5.08E-02 |
| | | Time | | 0.609 | 0.698 | 4.84E-05 |
| | | | Solid/liquid ratio | 0.127 | 0.106 | 1.29E-04 |

P value indicates significance analysis of difference using one-way analysis of variance test.

tyrosine/tryptophan proteins (II, Em 220–290 nm/Ex 280–360 nm); polysaccharides (III, Em 300–330 nm/Ex 360–390 nm); humic acids (IV, Em 300–370 nm/Ex 420–460 nm); and fulvic acids (V, Em 220–240 nm/Ex 410–450 nm) (Wang and Zhang, 2010). In the formation of distillers grains, the solid residue left by fermentation of grains contains a complex mixture of humic acids, proteins, and carbohydrates of different molecular sizes and functional groups (Sadeghi et al., 2016). As shown in Fig. 1, the fluorophores indicative of polysaccharides (III) and humic acids (IV) were the predominant components of DG I HLPs. This supports the conclusion that partial fragmentation of the original biomass was the source of HLPs DOC.

Fig. S1 (Supplementary material) shows the EEM contour maps of different raw materials (DG I, DG-V15% and DG II) HLPs varying temperature from 100 °C to 200 °C, the duration from 1 h to 6 h and the solid/liquid ratio from 5% to 10%. All the EEMS contour maps in Fig. S1 (Supplementary material) indicate two similar peaks related to polysaccharide-like material and humic-like material. When the raw material was DG I, the fluorescence intensity of organic compounds in HLPs increased obviously with the increase of HTT temperature. The HLPs peak intensity of polysaccharide and humic acid is very weak at the low HTT temperature of 100 °C, and the release amount was very small, until reaching 150 °C. At HTT of 200 °C, fluorescence intensity reached a maximum. This is in agreement with previous findings that, above 200 °C, degree of hydrochar condensation increases, as indicated by decreasing O/C and H/C ratios (Parshetti et al., 2013; Sevilla and Fuertes, 2009). In addition, the fluorescence intensity of organic compounds in HLPs decreased slightly with the increase of HTT time. However, with the increase of solid-liquid ratio, the HLPs peak area increases and more organic matter dissolved. Each row shows a similar trend. In the images from the first to the second lines, under the same experimental conditions, each peak area of DG-V15% was smaller than DG I, indicating that the existence of vermiculite inhibited the dissolution of organic matter. Many studies have also proved that it may be that adding vermiculite increased organic matter adsorption onto solid products, thus reducing the organic matter dissolution in liquid phase. (Shi et al., 2020; Xu et al., 2021).

### 3.2. HTT inorganic nutrient release efficiency

Concentrations of $NH_4^+$-N, $NO_3^-$-N and $PO_4^{3-}$ in DG I HLPs ranged from 3.6 to 92.0%, 19.7–89.9%, and 24.3–72.9%, respectively (Fig. 2 and Table S2, Supplementary material). However, examination of the efficiencies of nutrient release via HTT are a better way to compare and optimize HTT conditions for obtaining high nutrient yields.

The greatest efficiency of $NH_4^+$-N and $NO_3^-$-N release by DG I were 92.1% and 89.9%, respectively, and occurred at HTT conditions of 200 °C, 6 h, and solid/liquid ratio of 5% (Fig. 2). Maximal $PO_4^{3-}$ release efficiency from DG I, however, occurred with shorter HTT times (89.9 and 94.3%, after 3.5 and 1 h, respectively). Much as with DOC, the addition of vermiculite inhibited the release of inorganic nutrients into the liquid phase. Compared to DG I HLPs, release efficiencies of $NH_4^+$-N and $NO_3^-$-N and $PO_4^{3-}$ from DG-V5% were lower for each HTT condition. An explanation for this might be that vermiculate initiated the precipitation of nutrients from solution. For example, dissolved phosphate and nitrogen was precipitated by the addition of aluminum and iron salts to sewage sludge (Becker et al., 2019). In addition, the lower pH of DG I HLPs, versus that of DG-V5% HLPs, may have catalyzed dehydration and decarboxylation reactions that release $NH_4^+$-N, as shown previously conclusion of (Mau et al., 2019). In contrast, at 200 °C, 6 h, and solid/liquid ratio 10%, the $NO_3^-$-N release efficiency of DG I (89.9%) was higher than that of DG-V5% (64.8%). This is likely because the negative charge of the vermiculite surface would have affinity for $NO_3^-$-N adsorption.

Temperature, duration and solid/liquid ratio also affect the release efficiency of inorganic nutrients during HTT. As shown in Fig. 2, taking the case of DG I, when the HTT time was 1 h and the solid/liquid ratio

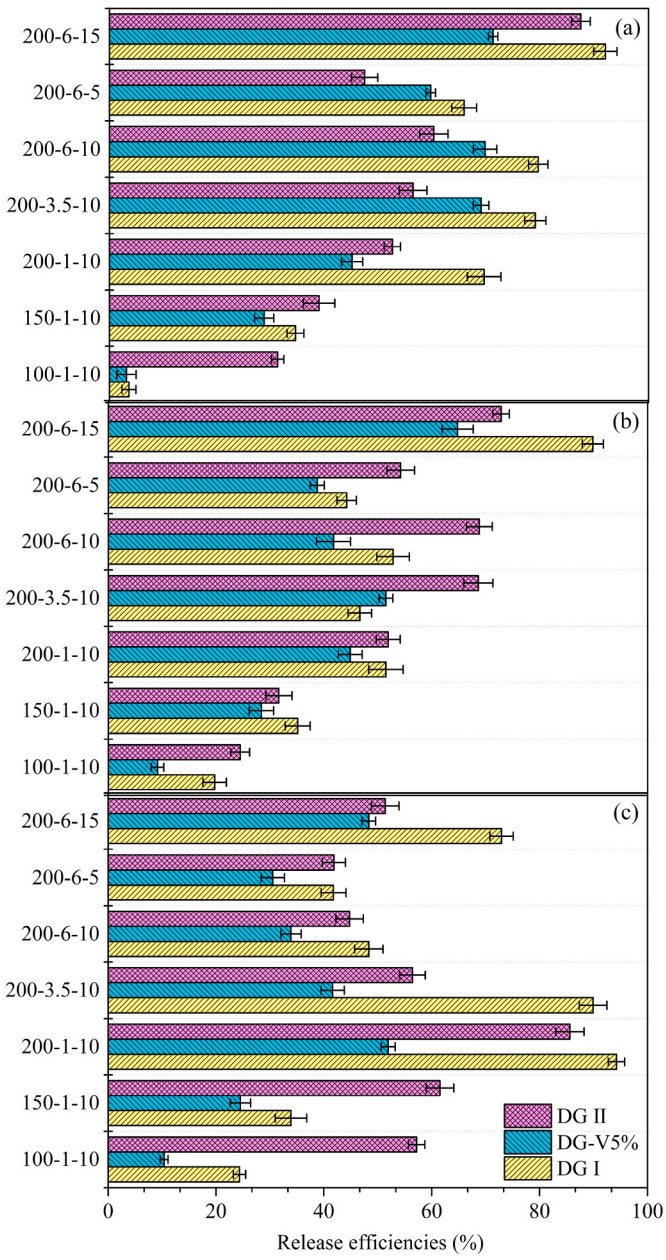


**Fig. 2.** Inorganic nutrient (a) $NH_4^+$-N (b) $NO_3^-$-N (c) $PO_4^{3-}$ release efficiencies (from biomass to HLPs) for DG I, DG-V5%, and DG II of varying temperature (100, 150, 200 °C), duration (1, 3.5, 6 h), and solid/liquid ratio (5, 10, 15%). Error bars represent one standard deviation.

was 10%, as the HTT temperature increased from 100 °C to 150 °C, the release efficiency of $NH_4^+$-N, $NO_3^-$-N, and $PO_4^{3-}$ increased by 20.9, 15.4, and 9.6%, respectively. With the increase of HTT temperature from 150 °C to 200 °C, the release efficiency of $NH_4^+$-N, $NO_3^-$-N and $PO_4^{3-}$ continued to increase (by 45.0, 16.4 and 60.4%, respectively). Some related studies have also demonstrated that HTT temperature is related to HLP inorganic nutrients (Song et al., 2019; Xiong et al., 2019). For example, Z. Wang et al. (2020) found that at between 180 and 260 °C, the retention of N in food waste feedstock decreased slightly with increasing HTT temperature.

Regardless of the feedstock type, at 200 °C HTT temperature and 10% solid/liquid ratio, release efficiency of $NH_4^+$-N increased, $PO_4^{3-}$ decreased, and $NO_3^-$-N did not change in a constant manor with HTT duration (Fig. 2). The increase in ammonium may be due to the progressive hydrolyzation of proteins, in distillers grains, and subsequent

deamination of the resultant amino acids over time, as has been proposed previously (Ekpo et al., 2016; Wu et al., 2018). The forms of $PO_4^{3-}$ in the distillers grains is complex, so there are some fluctuations in Fig. 2. Wu et al. (2018) found that orthophosphate ($PO_4^{3-}$) is the main form of P, but it is not stable. Heilmann et al. (2014) found that $Ca_3(PO_4)_2$ and $Mg_3(PO_4)_2$ minerals formed over the course of HTT of animal manures, enriching the solid product of HTT and depleting the HLP. In addition, solution pH is also likely to have a strong effect on the stability of these P.

### 3.3. Optimization of DGI HLPs nutrient recovery by RSM

Because the leaching rate of inorganic nutrients was found to be greatest from DG I than the other two raw materials RSM analysis was focused on this feedstock. Using principal component analysis equation (Eq. (2)), a new variable was obtained, $C_{PC}$, which were the HLPs nutrient ($NH_4^+$-N, $NO_3^-$-N and $PO_4^{3-}$) data (Table S3, Supplementary material) so as to facilitate the RSM analysis. The final equation obtained using the Design-Expert software, that described the dependencies of $C_{PC}$ on HTT temperature (A), duration (B) and solid/liquid ratio (C), was:

$$Y = 391.20 + 309.14 \times A + 16.98 \times B + 4.86 \times C - 2.20 \times AB + 22.32 \times AC - 3.00 \times BC + 14.31 \times A^2 + 37.84 \times B^2 - 13.44 \times C^2 \quad (4)$$

According to Eq. (4), increases in temperature and solid/liquid ratio have a predominantly positive impact on nutrient release ($C_{PC}$), whereas increasing duration results in negative effects on the removal. At the same time, ANOVA was used for analysis. The results are shown in Table S4. The model had a p-value and F-value of $<0.0001$ and 52.16, respectively, indicating that the regression was significant. The above description is in line with the RSM analysis requirements.

The interactive effects of the three independent parameters on HTT nutrient release were studied using RSM analysis. According to the analysis, for DG I, a maximum HLPs $C_{PC}$ concentration of 778.1 mg $L^{-1}$ could be obtained using the HTT conditions of 200 °C, for 6 h, and a solid/liquid ratio 15% (Fig. 3). The analysis also suggests that a greater amount of nutrients might have been extracted using HTT temperature even greater than 200 °C. However, if one had the goal of achieving maximum nutrient extraction while minimizing energy consumption (i.e HTT temperature and duration), that optimal condition occurred at 200 °C for 1 h. These results illustrate how response surface optimization design can be used to identify optimal HTT conditions for the extraction of inorganic nutrients from biomass.

### 3.4. Potential of HLPs as agricultural fertilizer

According to the previous experimental study, nutrient release in HLPs under the optimal reaction conditions: $NH_4^+$-N was 18.4 mg $L^{-1}$; $NO_3^-$-N was 0.14 mg $L^{-1}$; and $PO_4^{3-}$ was 14.2 mg $L^{-1}$. The HLPs nutrient release efficiency achieved in this study from distillers grains compares favorably with that of other studies using different biomass and HTT conditions (Table 2). While some other studies achieved higher levels of nutrient extraction, all of these were carried out at higher HTT temperatures, which would require greater inputs of energy. For example, HTT of cattle manure at 210 °C yielded 18.3 and 17.5 mg $g^{-1}$, $NH_4^+$-N and $PO_4^{3-}$, respectively (Wu et al., 2018). Some past studies have also shown that HLPs nutrients can promote plant growth (Wu et al., 2018). For example, use of HLPs to grow the microalgae *Chlorella*, resulted in

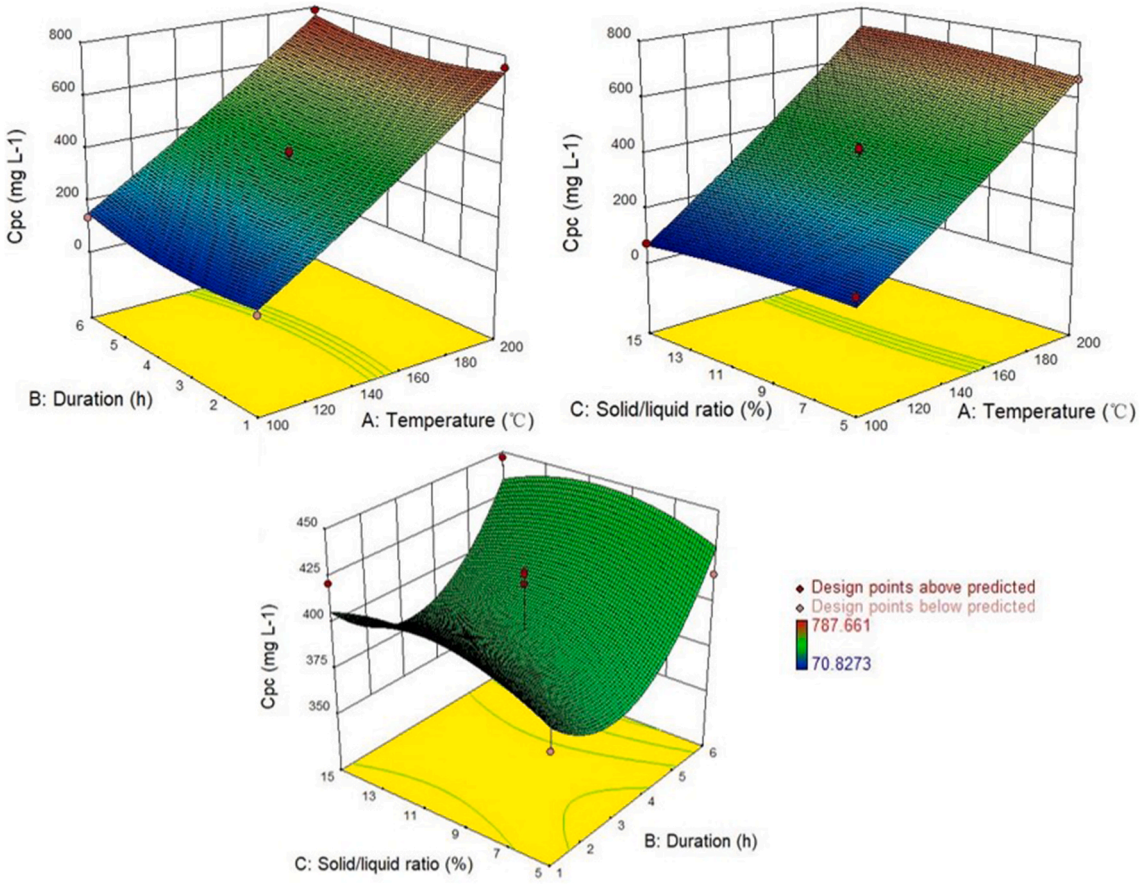


**Fig. 3.** Three-dimensional response surface plots of the interaction between HLP nutrients (principal component $C_{PC}$) and hydrothermal (a) temperature and duration; (b) temperature and solid/liquid ratio; (c) duration and solid/liquid ratio. The red dots represent the actual experimental values.

**Table 2**
Nutrient released by hydrothermal treatment of biomass observed in this and previous studies.

| Feedstock biomass | Hydrothermal treatment reaction conditions | $NH_4^+$-N (mg $g^{-1}$) | $NO_3^-$-N (mg $g^{-1}$) | $PO_4^{3-}$ (mg $g^{-1}$) | Reference |
|---|---|---|---|---|---|
| DG I | 200 °C for 1 h, solid-liquid ratio 10%. | 18.4 | 0.14 | 14.2 | This Study |
| Microalgae | 200 °C for 40 min 200 °C for 40 min | 8.9 | 1.4 | 4.7 | Du et al. (2012) |
| Straw digestate | 220 °C for 185 min | 0.7 | 0.05 | 2.1 | Funke (2015) |
| Corn digestate | 220 °C for 185 min | 0.7 | 0.02 | 0.2 | |
| Cattle manure | 210 °C for 1 h, solid-liquid ratio 10% | 18.3 | – | 17.5 | Wu et al. (2018) |
| Swine manure | 280 °C for 30 h, solid-liquid ratio 0.1 g/mL | 23.7 | 3.7 | 3 | Xiong et al. (2019) |
| Woody sawdust | 220 °C for 60 min | 14.6 | 2.6 | 15.1 | Wang et al. (2020) |
| Food waste | 220 °C for 60 min | 13.8 | 33.7 | 1.7 | |
| Poultry litter | 200 °C, solid-liquid ratio 1/3 | 1.9 | – | 0.4 | Mau et al. (2019) |
| | 250 °C, solid-liquid ratio 1/3 | 1.6 | – | 1.9 | |

faster algal growth over 4 days compared to BG-11 (a commercially available medium), showing that HLPs are nutrient solution (Du et al., 2012). In another study, diluted bagasse HLPs promoted the growth of roots and stems in maize and tomato seedlings (Fregolente et al., 2019). HLPs were also shown to support lettuce growth when it was used as fertilizer treatment at later stages of crop growth (Mau et al., 2019). All these indicated that HLPs have a good effect on fertility and promoting plant growth.

## 4. Conclusions

Results of this study confirm that the properties of HLPs were controlled by process conditions, particularly temperature, but also HTT duration and solid/liquid ratio. For DG I, response surface analysis, inorganic nutrients extraction was determined to occur at HTT conditions of 200 °C, for 1 h, and using a liquid-solid ratio 10%, which further indicated that higher HTT temperatures would increase nutrient extraction. While the addition of vermiculite not only reduces the nutrient extraction from distillers grains, but also slows the release rate of nutrients and organic acids during the distillers grains HTT. Results of this study suggest that HLPs has comprehensive and abundant nutrition. It met the needs of plant growth and could be used as plant nutrient solution. However, there are few practical application examples of HLPs at present, and whether it is feasible in large-scale production and application still needs follow-up tests.

## CRediT authorship contribution statement

**Qingya Xu:** Conceptualization, Methodology, Formal analysis, Investigation, Resources, Data curation, Writing – original draft. **Taoze Liu:** Conceptualization, Validation, Resources, Writing – review & editing, Visualization, Supervision, Project administration, Funding acquisition. **Bangyu Liu:** Investigation, Resources, Writing – review & editing. **Hongguang Cheng:** Writing – review & editing. **Cheng Yang:** Writing – review & editing. **Bing Wang:** Writing – review & editing. **Andrew R. Zimmerman:** Writing – review & editing. **Bin Gao:** Validation, Writing – review & editing.

## Declaration of competing interest

The authors declare that they have no known competing financial interests or personal relationships that could have appeared to influence the work reported in this paper.

## Acknowledgments

This work was partially supported by the Natural Science Foundation of China [42167067, 41930863].

## Appendix A. Supplementary data

Supplementary data to this article can be found online at https://doi.org/10.1016/j.jenvman.2022.115275.

## References

Becker, G.C., Wüst, D., Köhler, H., Lautenbach, A., Kruse, A., 2019. Novel approach of phosphate-reclamation as struvite from sewage sludge by utilising hydrothermal carbonization. J. Environ. Manag. 238, 119–125.
Du, Z., Hu, B., Shi, A., Ma, X., Cheng, Y., Chen, P., Liu, Y., Lin, X., Ruan, R., 2012. Cultivation of a microalga Chlorella vulgaris using recycled aqueous phase nutrients from hydrothermal carbonization process. Bioresour. Technol. 126, 354–357.
Ekpo, U., Ross, A.B., Camargo-Valero, M.A., Williams, P.T., 2016. A comparison of product yields and inorganic content in process streams following thermal hydrolysis and hydrothermal processing of microalgae, manure and digestate. Bioresour. Technol. 200, 951–960.
Fregolente, L.G., Miguel, T.B.A.R., de Castro Miguel, E., de Almeida Melo, C., Moreira, A. B., Ferreira, O.P., Bisinoti, M.C., 2019. Toxicity evaluation of process water from hydrothermal carbonization of sugarcane industry by-products. Environ. Sci. Pollut. Res. 26, 27579–27589.
Funke, A., 2015. Fate of plant available nutrients during hydrothermal carbonization of digestate. Chem. Ing. Tech. 87, 1713–1719.
He, C., Wang, K., Giannis, A., Yang, Y., Wang, J., 2015. Products evolution during hydrothermal conversion of dewatered sewage sludge in sub- and near-critical water: effects of reaction conditions and calcium oxide additive. Int. J. Hydrogen Energy 40, 5776–5787.
Heilmann, S.M., Molde, J.S., Timler, J.G., Wood, B.M., Mikula, A.L., Vozhdayev, G.V., Colosky, E.C., Spokas, K.A., Valentas, K.J., 2014. Phosphorus reclamation through hydrothermal carbonization of animal manures. Environ. Sci. Technol. 48, 10323–10329.
Huang, R., Wang, X., Xing, B., 2019. Removal of labile arsenic from flooded paddy soils with a novel extractive column loaded with quartz-supported nanoscale zero-valent iron. Environ. Pollut. 255, 113249.
Joel Reyes-Cabrera, R.G.L.J., 2017. Differences in biomass and water dynamics between a cotton-peanut rotation and a sweet sorghum bioenergy crop with and without biochar and vinasse as soil amendments. Field Crop. Res. 214, 123–130.
Katsuyama, M., Ohte, N., 2002. Determining the sources of stormflow from the fluorescence properties of dissolved organic carbon in a forested headwater catchment. J. Hydrol. (Amst.) 268, 192–202.
Kawamoto, H., 2017. Lignin pyrolysis reactions. J. Wood Sci. 63, 117–132.
Köchermann, J., Görsch, K., Wirth, B., Mühlenberg, J., Klemm, M., 2018. Hydrothermal carbonization: temperature influence on hydrochar and aqueous phase composition during process water recirculation. J. Environ. Chem. Eng. 6, 5481–5487.
Kumar, J.W.G.V., 2020. Recent trends in biochar production methods and its application as a soil health conditioner: a review. SN Appl. Sci. 2, 1307.
Li, L., Flora, J.R.V., Berge, N.D., 2020. Predictions of energy recovery from hydrochar generated from the hydrothermal carbonization of organic wastes. Renew. Energy 145, 1883–1889.
Li, Y., Tsend, N., Li, T., Liu, H., Yang, R., Gai, X., Wang, H., Shan, S., 2019. Microwave assisted hydrothermal preparation of rice straw hydrochars for adsorption of organics and heavy metals. Bioresour. Technol. 273, 136–143.
Lima, I., Bigner, R., Wright, M., 2017. Conversion of sweet sorghum bagasse into value-added biochar. Sugar. Tech. 19, 553–561.
Lucas Raimundo Bento, C.A.M.O., Benedito Moreira, S.M.A.P., Bisinoti, M.C., 2020. Humic extracts of hydrochar and Amazonian Dark Earth: molecular characteristics and effects on maize seed germination. Sci. Total Environ. 708, 135000.
Ma, L., Su, X., Xi, Y., Wei, J., Liang, X., Zhu, J., He, H., 2019. The structural change of vermiculite during dehydration processes: a real-time in-situ XRD method. Appl. Clay Sci. 183, 105332.
Mau, V., Neumann, J., Wehrli, B., Gross, A., 2019. Nutrient behavior in hydrothermal carbonization aqueous phase following recirculation and reuse. Envion. Sci. Technol. 53, 10426–10434.
Mazloomi, F., Jalali, M., 2019. Effects of vermiculite, nanoclay and zeolite on ammonium transport through saturated sandy loam soil: column experiments and modeling approaches. Catena 176, 170–180.
Minoglou, M., Komilis, D., 2018. Describing health care waste generation rates using regression modeling and principal component analysis. Waste Manag. 78, 811–818.
Nascimento, M., Soares, P.S.M., Souza, V.P.D., 2009. Adsorption of heavy metal cations using coal fly ash modified by hydrothermal method. Fuel 88, 1714–1719.

Oliveira, J.F.D., Fia, R., Fia, F.R.L., Rodrigues, F.N., Matos, M.P.D., Siniscalchi, L.A.B., 2020. Principal component analysis as a criterion for monitoring variable organic load of swine wastewater in integrated biological reactors UASB, SABF and HSSF-CW. J. Environ. Manag. 262, 110386.
Parshetti, G.K., Kent Hoekman, S., Balasubramanian, R., 2013. Chemical, structural and combustion characteristics of carbonaceous products obtained by hydrothermal carbonization of palm empty fruit bunches. Bioresour. Technol. 135, 683–689.
Pisa, C., Wuta, M., Muchaonyerwa, P., 2020. Effects of incorporation of vermiculite on carbon and nitrogen retention and concentration of other nutrients during composting of cattle manure. Bioresour. Technol. Rep. 9, 100383.
Ramesh, S., Sundararaju, P., Banu, K., Karthikeyan, S., Doraiswamy, U., Soundarapandian, K., 2019. Hydrothermal carbonization of arecanut husk biomass: fuel properties and sorption of metals. Environ. Sci. Pollut. Res. Int. 26, 3751–3761.
Reza, M.T., Andert, J., Wirth, B., Busch, D., Pielert, J., Lynam, J.G., Mumme, J., 2014. Hydrothermal carbonization of biomass for energy and crop production. Appl. Bioenergy 1, 1.
Román, S., Ledesma, B., Álvarez, A., Coronella, C., Qaramaleki, S.V., 2020. Suitability of hydrothermal carbonization to convert water hyacinth to added-value products. Renew. Energy 146, 1649–1658.
Sadeghi, S.H., Hazbavi, Z., Harchegani, M.K., 2016. Controllability of runoff and soil loss from small plots treated by vinasse-produced biochar. Sci. Total Environ. 541, 483–490.
Sevilla, M., Fuertes, A.B., 2009. The production of carbon materials by hydrothermal carbonization of cellulose. Carbon 47, 2281–2289.
Sharma, S., Aygun, A., Simsek, H., 2020. Electrochemical treatment of sunflower oil refinery wastewater and optimization of the parameters using response surface methodology. Chemosphere 249, 126511.
Shi, W., Ju, Y., Bian, R., Li, L., Joseph, S., Mitchell, D.R.G., Munroe, P., Taherymoosavi, S., Pan, G., 2020. Biochar bound urea boosts plant growth and reduces nitrogen leaching. Sci. Total Environ. 701, 134424.
Song, C., Zheng, H., Shan, S., Wu, S., Wang, H., Christie, P., 2019. Low-temperature hydrothermal carbonization of fresh pig manure: effects of temperature on characteristics of hydrochars. J. Environ. Eng. 6, 145.
Sumida H, S.X., Sumida H, Y.K., 2013. Effects of hydrothermal process on the nutrient release of sewage sludge. Int. J. Wine Res. 3, 2.
Wang, T., Si, B., Gong, Z., Zhai, Y., Cao, M., Peng, C., 2020. Co-hydrothermal carbonization of food waste-woody sawdust blend: interaction effects on the hydrochar properties and nutrients characteristics. Bioresour. Technol. 316, 123900.
Wang, T., Zhai, Y., Zhu, Y., Li, C., Zeng, G., 2018. A review of the hydrothermal carbonization of biomass waste for hydrochar formation: process conditions, fundamentals, and physicochemical properties. Renew. Sustain. Energy Rev. 90, 223–247.
Wang, Z., Wu, Z., Tang, S., 2009. Characterization of dissolved organic matter in a submerged membrane bioreactor by using three-dimensional excitation and emission matrix fluorescence spectroscopy. Water Res. 43, 1533–1540.
Wang, Z., Zhai, Y., Wang, T., Peng, C., Li, S., Wang, B., Liu, X., Li, C., 2020. Effect of temperature on the sulfur fate during hydrothermal carbonization of sewage sludge. Environ. Pollut. 260, 114067.
Wang, Z., Zhang, T., 2010. Characterization of soluble microbial products (SMP) under stressful conditions. Water Res. 44, 5499–5509.
Wu, K., Zhang, X., Yuan, Q., 2018. Effects of process parameters on the distribution characteristics of inorganic nutrients from hydrothermal carbonization of cattle manure. J. Environ. Manag. 209, 328–335.
Xiong, J., Pan, Z., Xiao, X., Huang, H., Lai, F., Wang, J., Chen, S., 2019. Study on the hydrothermal carbonization of swine manure: the effect of process parameters on the yield/properties of hydrochar and process water. J. Anal. Appl. Pyrol. 144, 104692.
Xu, Q., Liu, T., Li, L., Liu, B., Wang, X., Zhang, S., Li, L., Wang, B., Zimmerman, A.R., Gao, B., 2021. Hydrothermal carbonization of distillers grains with clay minerals for enhanced adsorption of phosphate and methylene blue. Bioresour. Technol. 340, 125725.
Yu, Y., Lei, Z., Yuan, T., Jiang, Y., Chen, N., Feng, C., Shimizu, K., Zhang, Z., 2017. Simultaneous phosphorus and nitrogen recovery from anaerobically digested sludge using a hybrid system coupling hydrothermal pretreatment with MAP precipitation. Bioresour. Technol. 243, 634–640.
Yujia Xiang, X.Y.Z.X., 2020. Fabrication of sustainable manganese ferrite modified biochar from vinasse for enhanced adsorption of fluoroquinolone antibiotics: effects and mechanisms. Sci. Total Environ. 709.